Dynamic Hepatobiliary SPECT: A Method for Tomography of a Changing Radioactivity Distribution

Bernard E. Oppenheim and John D. Krepshaw

Division of Nuclear Medicine, Department of Radiology, Indiana University School of Medicine, Indianapolis, Indiana

Dynamic single photon emission computed tomography (SPECT) of a changing radioactivity distribution can be performed with a rotating scintillation camera by acquiring several 360° studies and generating a new 360° study for which the acquisition time for every image is shifted to a single selected time. Following suppression of gallbladder filling with a fatty meal, dynamic SPECT of the hepatobiliary system was carried out by acquiring two successive studies with each head of a dual-headed camera within a 35-min period following injection of technetium-99m DISIDA. Each of the four acquired studies consisted of 60 images acquired at 6° intervals, spanning 360°. Time-shifted studies, each consisting of 60 images over 360°, were generated for times 9, 17, and 26 min postinjection. Transverse, sagittal, and coronal images were generated for each study. These images were artifact-free and demonstrated physiologic shifting of the radioactivity distribution over time. When gallbladder filling was not suppressed gross artifacts were obtained. This procedure permits examination of regional liver function and provides improved visualization of the biliary tree.

J Nucl Med 29:98–102, 1988

Dynamic single photon emission computed tomography (SPECT) refers to tomographic reconstruction of a radioactivity distribution that is changing during the time of data acquisition. It is the tomographic counterpart of a dynamic study, that is a series of images obtained over any appropriate time interval depicting a change in the distribution of radiopharmaceuticals (*1*). In studies performed with a rotating scintillation camera, dynamic SPECT is not readily accomplished because the reconstruction algorithms assume that the radioactivity distribution remains constant during data acquisition. Any variation in this distribution is liable to introduce artifacts into the reconstructed images. For example, such artifacts are produced by a rapidly filling bladder on a SPECT study of the hips (*2*).

In hepatobiliary studies performed with [^{99m}Tc]-DISIDA the tracer is taken up by the hepatocytes of the liver and gradually appears in the biliary system, and subsequently in the gallbladder and small bowel. The continually shifting distribution of radioactivity would introduce artifacts into SPECT images generated by conventional techniques. We have developed a method of time-shifting that utilizes multiple 360° data acquisitions with the rotating camera to generate high quality dynamic SPECT images of the hepatobiliary system. Furthermore, one may specify any time within a predetermined interval and generate images representing the radioactivity distribution at that time.

MATERIALS AND METHODS

We carried out computer simulations to demonstrate the effect of a changing radioactivity distribution on the reconstructed image (Fig. 1). A set of projections was made of a Gaussian-shaped hot spot superimposed on a uniform disk, to which Poisson random noise was added. The amplitude of the hot spot was fixed at twice the amplitude of the disk. An artifact-free image was reconstructed from these projections by the method of filtered backprojection (Fig. 1A). In a second set of projections, the amplitude of the hot spot was varied, beginning at 0 for the projection at 0°, and increasing by equal increments in successive projections, ending at four times the

Received Jan. 29, 1987; revision accepted Aug. 10, 1987.

For reprints contact: Bernard E. Oppenheim, MD, Div. of Nuclear Medicine, Indiana University School of Medicine, 926 West Michigan St., Indianapolis, IN 46223.

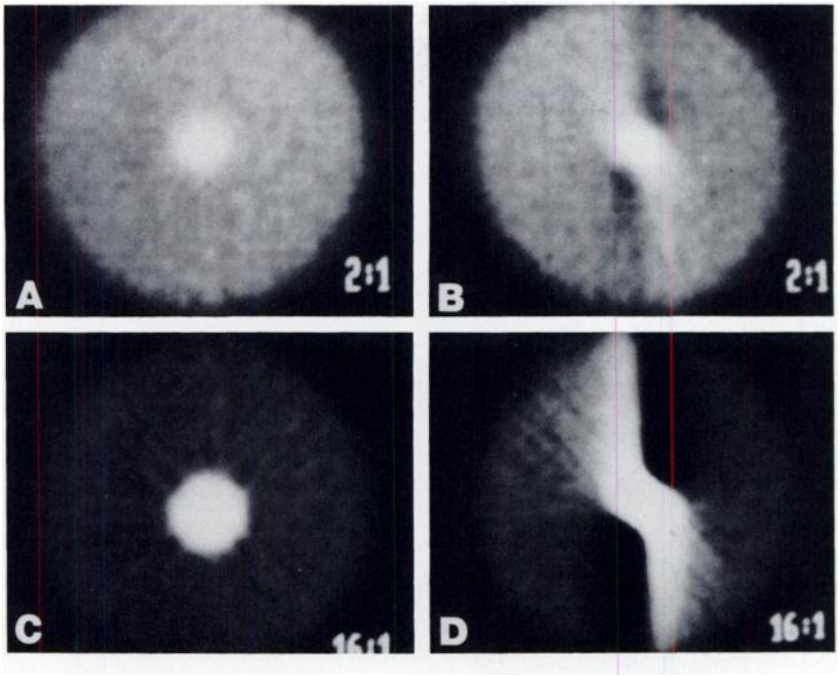

FIGURE 1
Computer simulations of artifact caused by changing radioactivity distribution. Reconstructions from projections of hot spot superimposed on uniform disk. A: Amplitude of hot spot fixed at twice that of disk. B: Amplitude of hot spot varies from zero to four times that of disk. C: Amplitude of hot spot fixed at 16 times that of disk. D: Amplitude of hot spot varies from zero to 32 times that of disk. Varying hot spot is distorted with hot and cold artifacts extending from it.

amplitude of the disk for the projection at 360°. The mean amplitude of the hot spot, which was twice that of the disk, occurred at 180°. In the reconstructed image the hot spot was distorted with tails of increased and decreased values extending from it (Fig. 1B). The artifacts became much more pronounced when the simulations were repeated with a varying hot spot having a mean amplitude 16 times that of the disk (Fig. 1D), while the reconstruction of the equivalent fixed hot spot was again artifact-free (Fig. 1C).

Beginning 1-min following the i.v. injection of 5 mCi [^{99m}Tc]DISIDA, a pair of 60 image studies of the abdomen was acquired over 360° with the two heads of a dual-headed scintillation camera* in 17 min. These were stored in the computer as 64 × 64 digital images. Following a 1.2-min interval for resetting the system, a second pair of 60 image studies was acquired and stored. Altogether 240 images were acquired in a 35 min interval, four at each of the 60 positions of the camera head.

A time-shifted study consisting of 60 images over 360°, equivalent to the images that would have been obtained by simultaneous acquisition at all positions at some selected time s, was generated as follows:

For each of the 60 positions, two images A and B, acquired at times a and b, were selected from the four images acquired at that position, where A and B were consecutively acquired and $a \leq s \leq b$. The time-shifted 64 × 64 image S was reconstructed for that position by weighted averaging of images A and B on a pixel-by-pixel basis using linear interpolation:

$$S = A(b - s)/(b - a) + B(s - a)/(b - a). \quad (1)$$

As an example, images at the 50° position (the sixth position imaged by the "red" head that was initially at 0°) were acquired by the "red" head at 1 min, 42 sec and at 19 min, 54 sec, while the "green" head (initially at 180°) acquired images at that position at 10 min, 12 sec and at 28 min, 24 sec into the study. To obtain reconstructions corresponding to the time s = 9 min, a time-shifted image corresponding to that time would be generated for every position. For the 50° position the two consecutively acquired images, one preceding and one following time s = 9 min, are the 1 min, 42 sec image (image A) and the 10 min, 12 sec image (image B). Using a = 102 sec, b = 612 sec, and s = 540 sec, Eq. (1) indicates that the time-shifted image S for that position would be formed by assigning a value to each pixel equal to the value for the corresponding pixel of image A multiplied by the weight 0.1412 plus the value for the corresponding pixel of image B multiplied by the weight 0.8588.

From the set of 60 time-shifted images, sets of 1-pixel-thick attenuation-corrected transverse, sagittal, and coronal slices were reconstructed using commercially available software.† Reconstructions were carried out with time shifting to times s = 9, 17, and 26 min from onset of data acquisition.

The study was performed in a healthy 48-yr-old male volunteer who had been given a fatty meal to keep the gallbladder from visualizing during data acquisition. In a second study on the same volunteer in which the gallbladder did visualize, inappropriate acquisition parameters allowed time-shifting only to the time s = 17 min.

RESULTS

Reconstructions from the study with nonvisualized gallbladder are shown in Figures 2 and 3. Transverse sections through the level of the common bile duct show that when the standard reconstruction algorithm is applied without time-shifting (Fig. 2A), the bile duct becomes badly distorted with artifactual regions of increased and decreased uptake adjacent to it, reminiscent of the artifacts demonstrated in Figure 1. The time-shifted images (Figs. 2B, C, and D) are free of such distortions and artifacts, although the high radioactivity concentration in the common bile duct has led to some

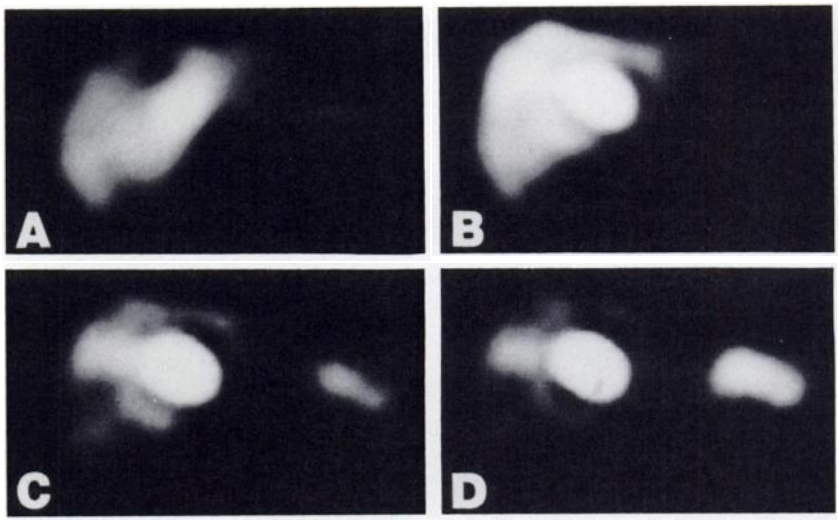

FIGURE 2
Dynamic hepatobiliary SPECT. Transverse sections through common bile duct. A: Reconstructed from 0–17 min acquisition without time-shifting. Common bile duct is distorted with associated hot and cold artifacts. B–D: Reconstruction from time-shifted images, with time-shifting to B: 9 min, C: 17 min, and D: 26 min. There is "ballooning" of common bile duct due to high radioactivity concentration. Images are otherwise undistorted and show gradual central progression of radioactivity. Progressive uptake is seen in loop of jejunum.

"ballooning" of the image of this structure. These images demonstrate passage of bile from the peripheral to the more central portions of the liver over time, along with increasing visualization of a loop of jejunum in which bile is progressively accumulating.

In the transverse, sagittal, and coronal tomographic images (Figs. 3B, C, and D), the bile ducts are visualized with greatly increased contrast compared with standard planar images, and their spatial configuration is much more readily appreciated than in the planar images (Fig. 3A).

Reconstructions from the study in which the gallbladder visualized (Fig. 4) demonstrate marked distortion in sections through the gallbladder. Sections which do not include the gallbladder are free from spatial distortion, but suffer from compression of the gray scale into a few gray levels.

DISCUSSION

Reconstruction algorithms generally assume that the projection data are consistent; that is, the data represent projections of the same object obtained at different angles. In reconstruction by filtered backprojection, each projection is altered in such a manner that when all the projections are backprojected, appropriate summation and cancellation will occur at every point in the reconstruction plane to yield an image that closely resembles the true radioactivity distribution (*3*) (for this discussion we ignore other sources of artifacts such as attenuation and scatter). If a changing radioactivity distribution is imaged with a rotating scintillation camera, then the image formed at each position represents the projection of a different radioactivity distribution. The projection data are inconsistent, and when the filtered projections are backprojected, inappropriate summations and cancellations occur in various regions of the reconstruction plane to yield an image that may contain bad distortions, as demonstrated in Figures 1, 2A, and 4D. Such distortions may be avoided by rapid imaging over all positions using a ring detector (*4,5*), a fixed camera with rotating tomographic collimator (*6*), or a rapidly rotating camera (*7*). These approaches

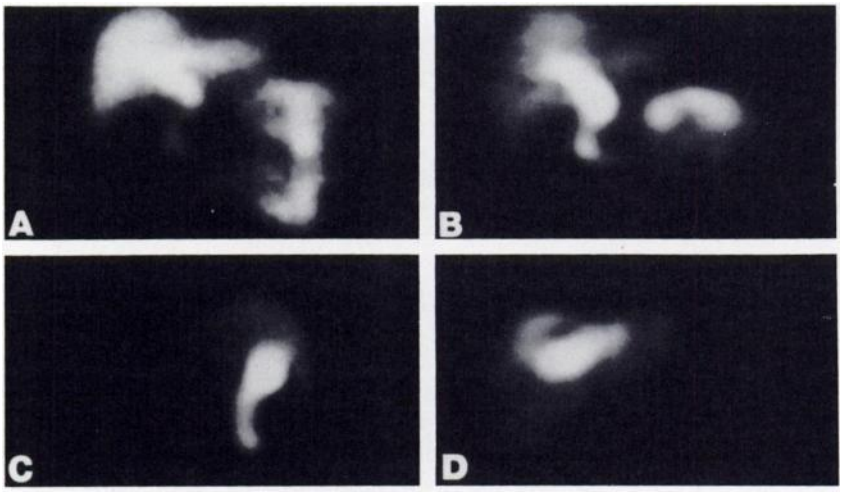

FIGURE 3
Planar versus SPECT hepatobiliary imaging. A: Anterior planar image, formed by summing four 0° images. Common bile duct not well delineated. B–D: Sections through common bile duct reconstructed from images time-shifted to 17 min. B: Coronal, C: Sagittal, and D: Transverse section (at bifurcation into left and right hepatic ducts). Visualization of duct greatly improved.

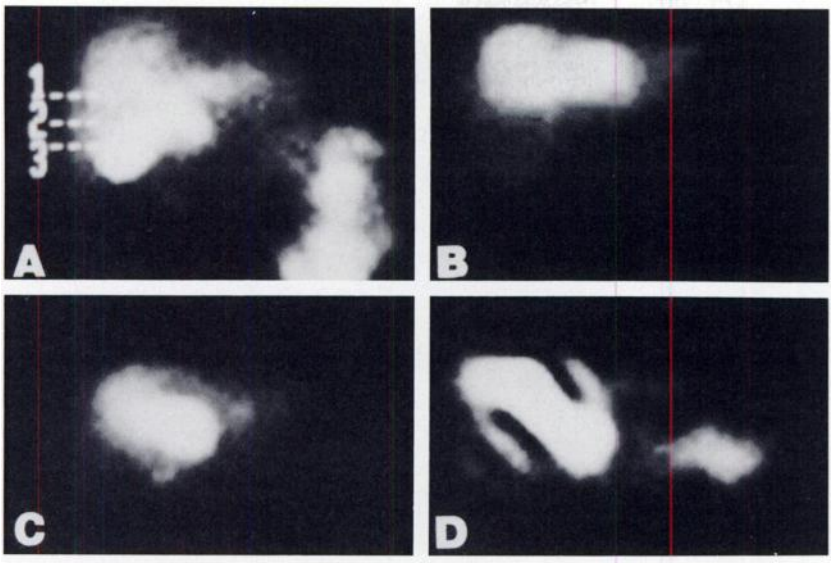

FIGURE 4
Effect of gallbladder visualization. A: Anterior planar image, formed by summing four 0° images. Three levels are indicated. B–D: Transverse sections at indicated levels reconstructed from images time-shifted to 17 min. Section through gallbladder demonstrates severe artifacts. Other sections undistorted but have compressed gray scale since software sets maximum brightness at hottest voxel in entire volume.

would be expected, however, to produce severely count-limited images due to short acquisition time.

The method of time-shifting presented here attempts to generate consistent sets of projection data from multiple conventionally-acquired studies. The method produces an image for every position of the camera head that represents the projection, at that position, of the radioactivity distribution as it would appear at a single selected time. The underlying concept is simple: if we have a number of images obtained from a single position at different times, and we assume that the radioactivity distribution changes linearly between successive imaging times, then an image at any intermediate time can be obtained by linear interpolation between two acquired images on a pixel-by-pixel basis. If we choose a single time and generate the corresponding image for each position of the camera head, then we will have produced a consistent set of images and the projection data obtained from them will be consistent. The only limitation here is that the chosen time cannot be earlier than the time of the initial image obtained at any position, nor later than the time of the final image obtained at any position. In the current study this permitted time-shifting to any time between 8.5 min and 26.5 min postinjection.

The assumption that the radioactivity distribution changes linearly between observations does not appear to be restricting. With our dual-headed system we imaged at a given position every 8.5 min, so that a nonlinear but continuous change would have only ~4–5 min to develop its maximum deviation from linearity. Only a nonlinearity of large magnitude might be expected to introduce a significant artifact. In all of our time-shifted reconstructions the liver parenchyma, common bile duct, and jejunum were reconstructed without apparent artifact. The gallbladder, whose intense activity totally dominated the image, was reconstructed with severe distortion, indicating that its changing activity pattern did not fulfill the linearity assumption. We know of no way to avoid this distortion, other than to suppress gallbladder filling by having the subject eat a fatty meal before dosing.

Biliary excretion occurred rapidly in the normal volunteer whose studies are presented here. A more prolonged acquisition period or perhaps some delay in beginning acquisition might be desirable for patients with slow excretion, if these patients could be identified in advance.

Since only a portion of the acquired information is used in generating a time-shifted reconstruction, image statistics are necessarily poorer than they would be if the radioactivity distribution were constant and all of the information could have been utilized. The statistics are improved somewhat by the weighted averaging of pairs of images. This is equivalent to an average increase in counting efficiency by a factor of ~1.6 (see Appendix). That is to say, if 3 million total counts were acquired by a single head in each revolution, then the method of time shifting would generate images comparable to those generated from a 4.8 million count acquisition using standard reconstruction techniques (ignoring distortion due to the changing radioactivity distribution).

The dual-headed camera has the advantage of doubling the count rate; however, in the step-and-shoot mode considerable time is wasted in movement and stabilization of the camera head. In our study, for each 10 sec of acquisition an additional 7 sec was spent in nonacquisition functions. A single-headed camera capable of continuous acquisition could have achieved results similar to ours, provided that it could complete each rotation within 8 min. For adequate angular resolution a continuous rotation system would probably have to frame images about every 3°. This would require

twice the amount of data storage and processing time compared with a step-and-shoot system in which images could be acquired at 6° increments, as we have done, but would not introduce any deterioration in the quality of reconstructed images.

The purpose of this paper is to demonstrate the feasibility of the method of time-shifting for accomplishing SPECT in situations in which the radioactivity distribution is changing. The clinical value of this procedure remains to be demonstrated. For hepatobiliary studies it provides the opportunity to evaluate regional liver function and to determine the pattern of bile excretion, as well as the ability to produce high-contrast images of the biliary tree in various orientations. The method might also be useful in reducing the bladder artifact frequently seen in SPECT studies of the hips (*2*).

APPENDIX

The method of time-shifting averages pairs of images acquired from the same position of the camera head. This improves counting efficiency by a variable amount, depending on the relative contribution of each image.

From Eq. (1) we have

$$C_S = (1 - k)C_A + kC_B (0 \leq k \leq 1),$$

where C_A and C_B are Poisson random variables representing the counts in a typical pixel of acquired images A and B, C_S is the counts in the corresponding pixel of time-shifted image S, and k is a constant dependent on the time selected for time-shifting.

Two random variables can be considered to be equivalently "noisy" if they have the same coefficient of variation (ratio of standard deviation to expected value). It follows that the random variable with expected value C and standard deviation $\sigma(C)$ is as "noisy" as the Poisson random variable with expected value $P = C^2/\sigma^2(C)$. Now

$$\sigma^2(C_S) = (1 - k)^2C_A + k^2C_B.$$

If we let $C_B = mC_A$ then from the above equation for C_S,

$$C_A = C_S/[1 + (m - 1)k]$$

Then

$$P = C_S^2/\sigma^2(C_S) = C_S\,[1 + (m - 1)k]/[(1 - k)^2 + mk^2].$$

The improvement in counting efficiency is the average value of P/C_S over the interval $0 \leq k \leq 1$. The result is dependent on the value of m (the change in counts between image A and image B). One can show by numeric integration that for values of m between 0.33 and 3.0, the average value of P/C_S ranges from 1.57 to 1.63. Thus the weighted averaging of pairs of images, as implemented by the method of time-shifting, produces images which are as "noisy", on the average, as the originally acquired images would be if they contained 1.6 times the actual counts.

NOTES

*(Rota Camera) Siemens Medical Systems, Inc, Des Plaines, IL.

†(A^3 Clinical Imaging System) Medical Data Systems, Ann Arbor, MI.

ACKNOWLEDGMENT

The authors thank Katie Natalie for her secretarial assistance in the completion of this manuscript.

REFERENCES

1. Blahd WH. Nuclear medicine, Second edition. New York: McGraw-Hill, 1971: 560–561.
2. Collier BD, Carrera GF, Johnson RP, et al. Detection of femoral head avascular necrosis in adults by SPECT. *J Nucl Med* 1985; 26:979–987.
3. Ter-Pogossian MM. Basic principles of computed axial tomography. *Semin Nucl Med* 1977; 7:109–127.
4. Bonte FJ, Stokely EM. Single-photon tomographic study of regional cerebral blood flow after stroke: concise communication. *J Nucl Med* 1981; 22:1049–1053.
5. Buell U, Moser EA, Schmiedek P, et al. Dynamic SPECT with Xe-133: Regional cerebral blood flow in patients with unilateral cerebrovascular disease: Concise communication. *J Nucl Med* 1984; 25:441–446.
6. Logan KW, Holmes RA. Missouri University multiplane imager (MUMPI): a high sensitivity rapid dynamic ECT brain imager [Abstract]. *J Nucl Med* 1984; 25:P105.
7. Nakamura K, Maeda H, Nakagawa T, et al. Evaluation of dynamic SPECT in the hepatobiliary scintigraphy [Abstract]. *J Nucl Med* 1983; 24:P99.